EasyChair Preprint

№ 6298

Reflecting Metasurface Unit Cell Design with Multi-Bit Azimuthal Control

James Rains, Jalil Ur Rehman Kazim, Lei Zhang, Qammer Abbasi, Muhammad Imran and Anvar Tukmanov

August 15, 2021

Reflecting Metasurface Unit Cell Design with Multi-Bit Azimuthal Control

James Rains, Jalil ur Rehman Kazim, Lei Zhang,
Qammer H. Abbasi, & Muhammad Imran
James Watt School of Engineering
University of Glasgow
Glasgow, UK
j.rains.1, j.kazim.1@research.gla.ac.uk
lei.zhang, qammer.abbasi, muhammad.imran@glasgow.ac.uk

Anvar Tukmanov
British Telecommunications PLC
Adastral Park
Ipswich, UK
anvar.tukmanov@bt.com

***Abstract*—This work proposes a phase-shifting unit cell for a reconfigurable intelligent surface capable of exhibiting 7 discrete reflection phase shifts at 3.75 GHz. Sets of PIN diode-loaded unit cells are addressed column-wise to realise azimuthal electromagnetic transformation capabilities with a simple, vialess feeding mechanism. Simulated results utilising manufacturer's component data suggest a desirable average reflection loss of 1 dB. A particle swarm optimisation algorithm is employed to realise reflection phase uniformity. Oblique incidence performance is investigated, revealing desirable phase shift resolution versus incidence angle beyond 40° for TM-polarised waves.**

***Index Terms*—reconfigurable metasurfaces, reconfigurable intelligent surfaces, digital metasurfaces**

I. Introduction

Dynamic control over existing electromagnetic (EM) waves in wireless propagation environments has recently been of great interest to researchers and industry [1]. Reconfigurable intelligent surfaces (RISs) can passively manipulate EM waves to the benefit of communication networks without injecting more EM energy into the system or employing additional RF chains.

RISs may be pivotal in facilitating the realisation of smart radio environments (SREs), the aim of which is to create a fully programmable propagation environment that is capable of fulfilling multiple network functions, including wireless coverage enhancement, environmental sensing, wireless power transfer, and blocking unauthorised users, whilst offering ease of integration into existing physical and network environments [2]. Meanwhile, SREs must ensure efficient use of the spectrum and available transmission power through joint optimisation of the transmitters, receivers, and the propagating environment. It should be noted that control of the wireless propagation environment by itself is not a new phenomenon, as relays have provided this functionality for some time, albeit with increased cost and power consumption [3].

RISs are electrically thin and transversally electrically large composite structures. RISs achieve their wave transformation capability by acting as an impedance discontinuity whose surface-averaged susceptibility can be varied according to the tunable loads of their constituent sub-wavelength unit cell (UC) elements [1]. The nature of the available EM transformations is geometry-specific and band-limited, with several recent works realising reconfigurable anomalous reflection, beam focusing, polarisation switching, and even magnetless nonreciprocity [4][5][6].

In the microwave regime, control of the phase shifting properties of RIS UCs is commonly achieved by embedding within them semiconductor-based components, such as varactors and positive-intrinsic-negative (PIN) diodes, as well as RF micro-electromechanical system (RF-MEMS) switches [4]. By bridging gaps made in UC resonators with varactor diodes, it is possible to alter the capacitance and therefore the effective electrical length of the resonators, thereby altering the resonant frequency and consequently the reflection phase shift over a continuous range. Similarly, switches, such as RF-MEMS and PIN diodes, can be utilised for connecting and isolating sections of a resonator to the same effect for quantised phase control.

Digital metasurfaces (DMSs) [7], where the reflection phase behaviour is quantised into digital bits, have been shown to offer resilient EM manipulation capabilities even with a phase steps as coarse as a single bit $\phi_r \in [-90^\circ, 90^\circ]$. Quantisation of the UC reflection phase has been shown to reduce UC complexity and increase bandwidth compared to a continuous 360° phase range [8]. A 1-bit phase response facilitates ease in implementing biasing circuitry, where a UC can be equipped with a single PIN diode to provide the two required states.

Subwavelength square microstrip patches equipped with PIN diodes, connected to ground through vias, are often employed for DMSs. The resulting response when the PIN diode is reverse-biased resembles that of an artificial magnetic conductor (AMC) with in-phase reflection, whilst the forward-biased state provides out-of-phase reflection [9][5]. Extending this concept, achievable reflection phase resolution can be improved by introducing a second active element such that 4 discrete phase states are achieved in a 2-bit fashion (such as $\phi_r \in [-135^\circ, -45^\circ, 45^\circ, 135^\circ]$) [6]. For instance, the angle-insensitive column-controlled irregular hexagon-based DMS demonstrated by Zhang et al. [6] utilised 2 PIN diodes per UC to demonstrate nonreciprocity through space-time coding. The

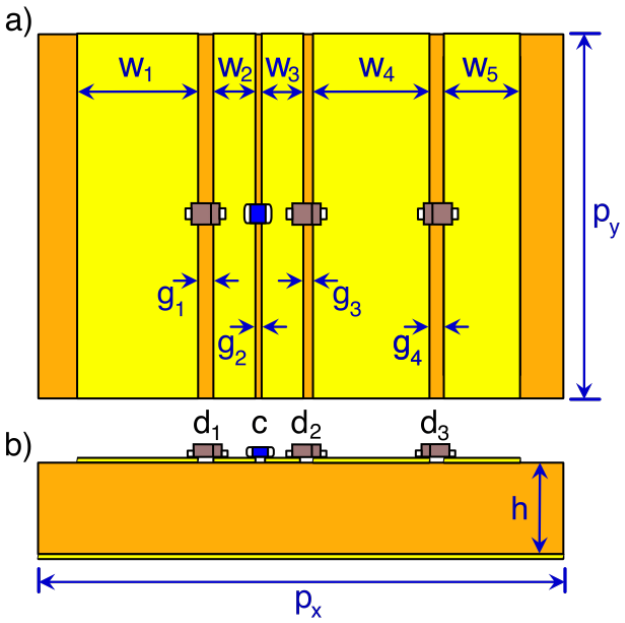

Fig. 1. Proposed digital reflecting metasurface unit cell. Above view (a) and cut view (b). Dimensions for 3.75 GHz operation are provided in table I. PIN diodes denoted d_1 to d_3 and DC blocking capacitor, C, acting as an RF short circuit at the operating frequency.

TABLE I
UNIT CELL DIMENSIONS

Parameter	Length (mm)	Parameter	Length (mm)
p_x, p_y	22.5, 14.7	w_1 to w_5	6, 0.9, 0.5, 6, 2.9
h	5	g_1 to g_4	0.9, 0.4, 1, 0.4

utilisation of 3 active elements for a 3-bit digital UC design has not yet been published, though Saifullah et al. recently simulated a column-controllable 3-bit UC design employing 4 PIN diodes [10].

Our work introduces a UC design capable of exhibiting discrete phase control beyond existing 2-bit designs with only a single additional active switching element while omitting vias, reducing fabrication complexity, and speeding up simulation time for optimisation. We additionally propose a new way of visualising the change in operating point with oblique incidence angle for reflecting UCs with several quantised phases.

II. Unit Cell Design

The proposed unit cell (UC) design can be seen in Fig. 1 with associated dimensions in table I. The UC consists of 5 microstrip patches directly connected to adjacent UCs above and below, and connected to neighboring patches via 3 PIN diodes, d_1 to d_3, and a DC blocking capacitor, C. The component arrangement enables common DC biasing signals to be applied to several unit cells in a column-wise fashion while maintaining an RF path through C, whose self-resonant frequency can be chosen such that it acts as a near-short circuit at the band of interest. The components employed here

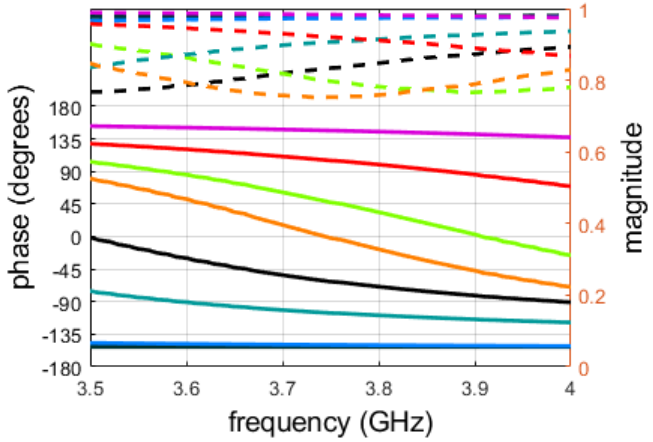

Fig. 2. Reflection magnitude (dashed lines, linear scale) and phase (solid lines, degrees) versus frequency for 8 unit cell configurations. The two bottom phase curves can be seen to be overlapping such that there are 7 available distinct phases.

are Skyworks SMP1321-040LF PIN diodes and an AVX U-Series 3.6 pF 0402 capacitor. The patches are mounted on a grounded F4BM-2 substrate with $\epsilon_r = 2.65$ and $tan\delta = 0.001$.

The UC was simulated with the commercial software CST Studio Suite employing the frequency domain solver with periodic boundary conditions. The PIN diodes were factored into the simulation by employing discrete ports at the component locations such that the system resembled a 4-port network (i.e., the incident wave and 3 PIN diode ports). This was followed by post-processing in which the reflection responses for the 8 PIN diode configurations were obtained by substituting the manufacturer-provided S-parameters in a similar fashion to Perruisseau-Carrier et al. [11] in their MEMS-based UC design. The S-parameters of the DC blocking capacitor were included in the simulation as lumped elements. A 5 mA biasing current was assumed for the *on* condition of the PIN diodes, while a 0 V voltage was simulated for the *off* condition. The UC was optimised for 3.75 GHz operation and the resulting phase and magnitude responses for the 8 biasing configurations can be seen in Fig. 2, where the available phase values at the centre frequency are $\phi_r \in [-150°, -104°, -60°, 0°, 49°, 107°, 148°]$. The resulting average reflection loss is 1 dB, with the largest loss at the 0° state of 2.5 dB. The losses are attributed mostly to the finite resistance of the PIN diodes.

III. Achieving Distinct Configurations

Compared to lower resolution UC designs, achieving sufficiently distinct reflection characteristics between diode configurations whilst minimising the UC complexity is challenging. Ideally, for each additional bit of resolution, it should be possible to utilise a single additional active element such that additional losses and configuration network complexity are minimised. However, without additional degrees of freedom it is necessary to find an exact set of parameters in an increasingly complex UC to satisfy the desired set of reflection

responses. Manual tuning of these parameters is prohibitively time consuming when attempting to align 8 phase states, since a change in a single parameter can affect all states at once.

We have utilised a particle swarm optimisation (PSO) algorithm to determine the parameter values due to its simplicity and the real-valued nature of the parameters [12]. PSO is a population-based optimisation algorithm whose population members, known as *particles*, each consisting of a set of parameters subject to optimisation. These particles collectively work to minimise a cost function through knowledge of the current global and their own local best set of parameter values. This is a technique that has been described as mimicking the way insect colonies cooperate to find food [13], with each member of the colony changing its search pattern according to the knowledge accumulated by themselves and the colony as a whole.

We have based our PSO implementation on the work by [11]. In this design, the substrate thickness, h, was fixed at $5\ mm$ while the 11 remaining parameters were subject to optimisation. The aim of the algorithm was to maximise the uniformity of the set of phase shifts about the operating frequency whilst minimising the reflection loss. One measure of phase shift uniformity utilised for discretely tunable reflecting UC designs is that of the equivalent bit number, N_{bit}, defined as:

$$N_{bit} = \log_2\left(\frac{360}{\sqrt{12}\sigma_p}\right) \tag{1}$$

$$\sigma_p = \sqrt{\frac{\sum_{m=1}^{M}(\Delta\phi_m)^3}{12 \times 360}} \tag{2}$$

where σ_p is the phase standard deviation for M configurations and $\Delta\phi_m$ are the phase differences between respective adjacent phase values. N_{bit} is a figure of merit and is useful for visualising the operating point of the digital UC. For example, a 4-state reflecting UC with 90° phase separation has an N_{bit} of 2 about its centre frequency, with N_{bit} typically reducing when moving away from this frequency. For instance, Luyen et al. [8] defined a working bandwidth of a 2-bit reflecting UC as the region where N_{bit} is 1.7 or higher while maintaining losses below 1 dB. For the reflection response in Fig. 2, the equivalent bit number at 3.75 GHz is 2.75 due to only achieving 7 instead of 8 distinct phase shifts. This response provides an acceptable improvement over 2-bit designs, with 3 additional available phases interpolating the 90° steps.

The PSO algorithm is summarised in Fig. 3. To begin, a population of particles is generated, each of which consists of a set of randomly generated parameter values for patch widths w_1 to w_5, patch spacing g_1 to g_4, and UC periodicities p_x and p_y within practical constraints. The main loop ensues, consisting of calculating the cost functions for each set of parameter values, followed by updating the local and global best sets of parameters for each particle, adjusting each particle's velocity based on these best values, followed by updating the particle positions (i.e., the associated parameter values) based on the respective velocities. The main loop repeats until convergence.

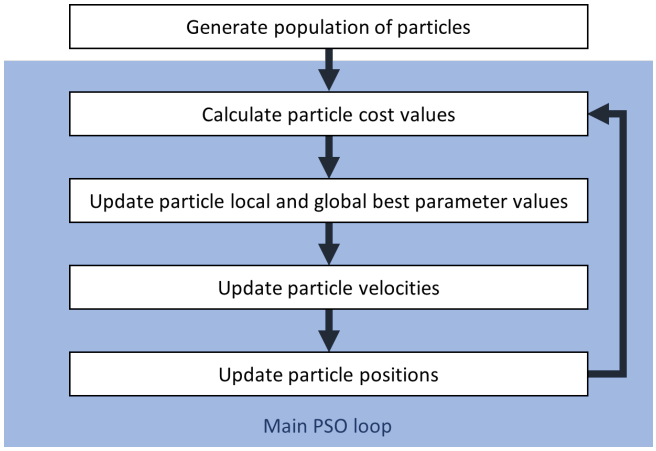

Fig. 3. Chart showing particle swarm optimisation algorithm employed for optimisation of the set unit cell reflection responses. Adapted from [12].

The cost function of the PSO algorithm was chosen as (3), where $\overline{\Gamma}(i)$ is the mean reflection magnitude for the 8 PIN diode configurations of particle i. Coefficients α_1 and α_2 were chosen as 1.5 and 0.5, respectively.

$$f_{cost}(i) = \alpha_1(3 - N_{bit}(i)) + \alpha_2(1 - \overline{\Gamma}(i)) \tag{3}$$

In order to reduce computation time on processing the set of parameters for each particle, a single frequency point was simulated for the 4-port network. For the UC geometry explored here, the PSO algorithm produced the 7 phase state result of Fig. 2 to maximise N_{bit}, though was also capable of producing 8 distinct states whose spacing was less desirable on approaching $\pm 180^\circ$. The optimised periodicity along the principal UC polarisation was $22.5\ mm$, resulting in under $\lambda_0/3$ UC spacing in the operating region.

IV. Oblique Incidence Performance

Due to its electrically thin nature, the proposed UCs predominantly interact with the tangential electric and magnetic components of incident waves and their ratio, the characteristic impedance seen at the surface, changes with incidence angle. The change in operating point (i.e., the N_{bit} maximum) with elevation incidence angle, θ_i, and polarisation has been plotted in Fig. 4(a), where Fig. 4(b) denotes the relevant coordinate system. The reflection response of the proposed UC varies according to the polarisation and there is a notable shift of the desired reflection response upwards in frequency when subject to a obliquely arriving TE wave. This shift is manifested in the phase values of the set of UC states appearing to group closer together at the operating frequency. The TE wave operating point can be seen to shift from 3.75 GHz at $\theta_i = 0^\circ$ to 4.15 GHz at $\theta_i = 45^\circ$. For TM waves at $\phi_i = 0^\circ$, this apparent shift in operating region is less pronounced.

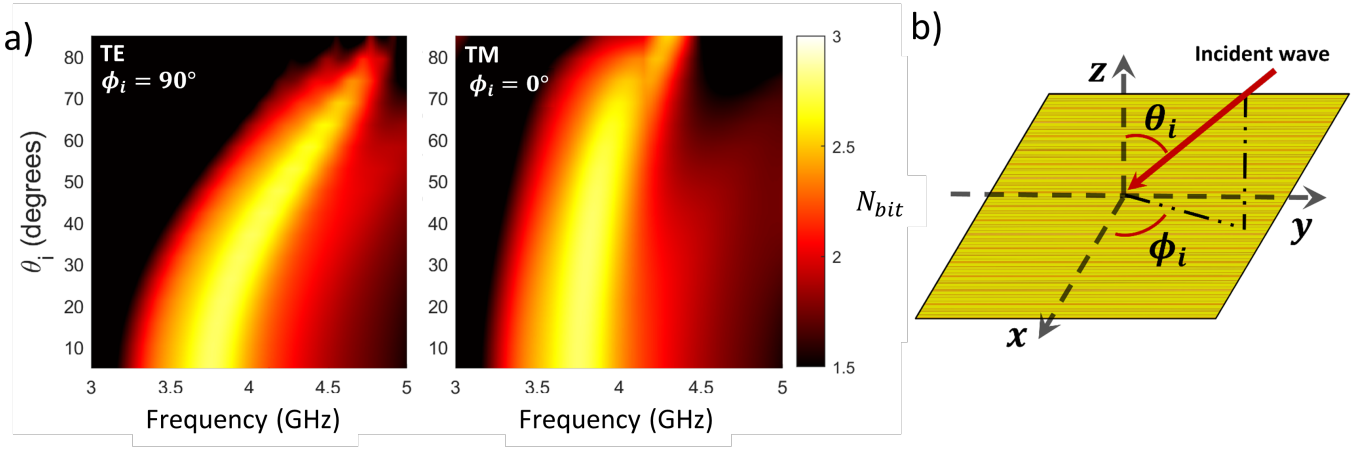

Fig. 4. Oblique incidence effects on the achievable phase resolution, N_{bit}, of the proposed unit cell design. (a) oblique incidence effects on the operating point of the unit cell design for TE and TM polarisations. (b) diagram showing oblique incidence measurement coordinate system superimposed on a tile of proposed units cells, aligned such that the PIN diodes are along the x axis. A high value of N_{bit} is desirable as it represents greater uniformity in the set of available phase responses.

V. Conclusion

The goal of this article was to highlight avenues for achieving high resolution wave transformation control with a minimal number of components and a low complexity configuration network. In the case of the column-driven UC design presented here, the biasing mechanism is to the detriment of any control in the elevation plane. Due to this limitation, for RIS-aided communication applications, the surface may be of utility either in scenarios where the base station antennas and UE are located in the same horizontal plane or where the base station antennas and UE virtual line of sight paths intercept the RIS at equal angles (i.e., the surface performs a combination of beamsteering in the azimuthal plane and specular reflection in the elevation plane). The proposed RIS is relatively cheap to produce due to the planar nature and simplicity of its design, thereby enabling cost-effective deployment of large RISs and their associated performance benefits over competing technologies [14]. A prototype with dimensions $13\lambda_0 \times 9\lambda_0$ has been fabricated, the wave transformation behaviour of which will be published in the near future.

References

[1] M. D. Renzo, A. Zappone, M. Debbah, M.-S. Alouini, C. Yuen, J. de Rosny, and S. Tretyakov, "Smart radio environments empowered by reconfigurable intelligent surfaces: How it works, state of research, and the road ahead," *IEEE Journal on Selected Areas in Communications*, vol. 38, pp. 2450–2525, nov 2020.

[2] E. Basar, M. D. Renzo, J. D. Rosny, M. Debbah, M.-S. Alouini, and R. Zhang, "Wireless communications through reconfigurable intelligent surfaces," *IEEE Access*, vol. 7, pp. 116753–116773, 2019.

[3] E. Björnson, Özgecan Özdogan, and E. G. Larsson, "Reconfigurable intelligent surfaces: Three myths and two critical questions,"

[4] J. P. Turpin, J. A. Bossard, K. L. Morgan, D. H. Werner, and P. L. Werner, "Reconfigurable and tunable metamaterials: A review of the theory and applications," *International Journal of Antennas and Propagation*, vol. 2014, pp. 1–18, 2014.

[5] C. Huang, C. Zhang, J. Yang, B. Sun, B. Zhao, and X. Luo, "Reconfigurable metasurface for multifunctional control of electromagnetic waves," *Advanced Optical Materials*, vol. 5, p. 1700485, sep 2017.

[6] L. Zhang, X. Q. Chen, R. W. Shao, J. Y. Dai, Q. Cheng, G. Castaldi, V. Galdi, and T. J. Cui, "Breaking reciprocity with space-time-coding digital metasurfaces," *Advanced Materials*, vol. 31, p. 1904069, aug 2019.

[7] T. J. Cui, M. Q. Qi, X. Wan, J. Zhao, and Q. Cheng, "Coding metamaterials, digital metamaterials and programming metamaterials,"

[8] H. Luyen, J. H. Booske, and N. Behdad, "2-bit phase quantization using mixed polarization-rotation/non-polarization-rotation reflection modes for beam-steerable reflectarrays," *IEEE Transactions on Antennas and Propagation*, pp. 1–1, 2020.

[9] J. ur Rehman Kazim, M. Ur-Rehman, M. Al-Hasan, I. B. Mabrouk, M. A. Imran, and Q. H. Abbasi, "Design of 1-bit digital subwavelength metasurface element for sub-6 GHz applications," in *2020 International Conference on UK-China Emerging Technologies (UCET)*, IEEE, aug 2020.

[10] Y. Saifullah, F. Zhang, G.-M. Yang, and F. Xu, "3-bit programmable reflective metasurface," in *2018 12th International Symposium on Antennas, Propagation and EM Theory (ISAPE)*, IEEE, dec 2018.

[11] J. Perruisseau-Carrier, F. Bongard, R. Golubovic-Niciforovic, R. Torres-Sánchez, and J. R. Mosig, "Contributions to the modeling and design of reconfigurable reflecting cells embedding discrete control elements," *IEEE Transactions on Microwave Theory and Techniques*, vol. 58, pp. 1621–1628, jun 2010.

[12] Z. Chen, *Handbook of antenna technologies*. Singapore: Springer Reference, 2016.

[13] D. Wang, D. Tan, and L. Liu, "Particle swarm optimization algorithm: an overview," *Soft Computing*, vol. 22, pp. 387–408, jan 2017.

[14] E. Bjornson, O. Ozdogan, and E. G. Larsson, "Intelligent reflecting surface versus decode-and-forward: How large surfaces are needed to beat relaying?," *IEEE Wireless Communications Letters*, vol. 9, pp. 244–248, feb 2020.